

Dynamics of modulated waves in a lossy modified Noguchi electrical transmission lineE. Kengne,¹ A. Lakhssassi,¹ and W. M. Liu²¹*Department of Computer Sciences and Engineering, University of Quebec at Outaouais, 101 St-Jean-Bosco, Succursale Hull, Gatineau(PQ), Canada J8Y 3G5*²*Beijing National Laboratory for Condensed Matter Physics, Institute of Physics, Chinese Academy of Sciences, Beijing 100190, People's Republic of China*

(Received 10 March 2015; revised manuscript received 18 May 2015; published 24 June 2015)

We study analytically the dynamics of modulated waves in a dissipative modified Noguchi nonlinear electrical network. In the continuum limit, we use the reductive perturbation method in the semidiscrete limit to establish that the propagation of modulated waves in the network is governed by a dissipative nonlinear Schrödinger (NLS) equation. Motivated with a solitary wave type of solution to the NLS equation, we use both the direct method and the Weierstrass's elliptic function method to present classes of bright, kink, and dark solitary wavelike solutions to the dissipative NLS equation of the network. Through the exact solitary wavelike solutions to the dissipative NLS equation, we investigate the effects of the dissipative elements of the network on wave propagation. We show that the wave amplitude decreases and its width increases when the dissipative element of the network increases. It has been also found that the dissipative element of the network can be used to manipulate the motion of solitary waves through the network. This work presents a good analytical approach of investigating the propagation of solitary waves through discrete electrical transmission lines and is very important for studying modulational instability.

DOI: [10.1103/PhysRevE.91.062915](https://doi.org/10.1103/PhysRevE.91.062915)

PACS number(s): 05.45.Yv, 84.40.Ua, 84.40.Az

I. INTRODUCTION

Because of its wide significance in a great variety of physical systems, the propagation of modulated waves has been the subject of considerable interest for many years, as, for example, in nonlinear optics [1–5]. On the other hand, discrete electrical transmission lines are very convenient tools to study the wave propagation in one-dimensional (1D) nonlinear dispersive media [5–19]. They have been applied to the study of thin-film and diffusion resistors, capacitors, and conductors and to the evaluation of undesirable interaction between different components of integrated circuits; moreover, discrete electrical transmission lines can be successfully used to simulate the characteristics of some active microcircuit elements, in particular, the field-effect transistors [6,7]. In particular, lossy transmission lines with nonlinear loads are very important for the study of and the design of high-speed electronic circuits [8]. Owing to the increasing frequencies and bit rates, one has to take the transmission line effects of the interconnections into account, for example, signal-delay, reflexion, attenuation, and cross talk [9]. Most recently, nonlinear transmission lines have proven to be of great practical use in extremely wide band (frequencies from dc to 100 GHz) focusing and shaping of signals (that is, changing certain features of incoming signals, such as the frequency content, pulse width, and amplitude), which is usually a hard problem [11]. In biomedical engineering, networks consisting of resistors, inductors, and capacitors, connected in series or in parallel, are used as an approximation of the nonlinear conservation law for blood flow in biological tissues [20–24].

Motivated by the qualitative and quantitative studies of properties of solitons in real nonlinear dispersive media, we aim in this paper to present a detailed calculation to predict the modulational instability (MI) and to evaluate quantitatively the dissipative effects on the envelope soliton in the modified

Noguchi electrical transmission line [25] taking into account the dissipation of the electrical components. The rest of the paper is organized as follows. In Sec. II we present a brief description of our model and write the basic equations of the lossy modified Noguchi electrical transmission line in Fig. 1. Using the reductive perturbation method in the semidiscrete limit [14,26], we establish in Sec. III that the dynamics of modulated waves in the lines is described by a dissipative nonlinear Schrödinger (NLS) equation. In Sec. IV we find analytical bright and dark or kink solitary wavelike solutions of the dissipative NLS equation of the network. With the help of analytical solutions, we investigate analytically the propagation of bright, dark, and kink solitary waves along the network in Sec. V. Finally, the main results are summarized in Sec. VI.

II. MODEL DESCRIPTION AND CIRCUIT EQUATIONS

The model under consideration is a lossy 1D modified discrete Noguchi electrical transmission line shown in Fig. 1 made of N identical unit cells. Each unit cell is modeled by a linear inductor L_1 in parallel with a linear capacitance C_S in the series branch and a linear inductor L_2 in parallel with a nonlinear capacitor C in the shunt branch. In order to take into account the dissipation of the network, a conductance G is connected in parallel with inductor L_2 , accounting for the dissipation of L_2 in addition with the loss of the nonlinear capacitor C . The nonlinear capacitor C consists of a reverse-biased diode with differential capacitance function of the voltage V_n across the n th capacitor. It is biased by a constant voltage V_b and depends on the voltage V_n , for low voltage, at cell n as [19]

$$C(V_b + V_n) = \frac{dQ_n}{dV_n} \simeq C_0(1 - 2\alpha V_n + 3\beta V_n^2), \quad (1)$$

where $C_0 = C(V_b)$ is the characteristic capacitance and $\alpha > 0$ and $\beta > 0$ designate the nonlinear coefficients of the electrical

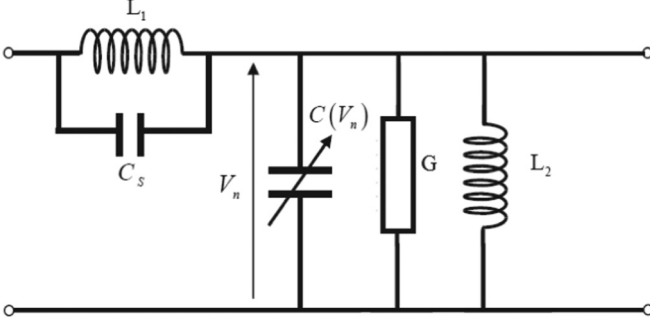


FIG. 1. Schematic representation of the elementary cell of the lossy 1D modified discrete Noguchi electrical transmission line. The network possesses N identical unit cells.

stored charge Q_n ; the subscript n stands for the number of cells in the network. During the computation, we use the following network parameters [10,19]: $L_1 = 200 \mu\text{H}$, $L_2 = 470 \mu\text{H}$, $V_b = 2 \text{ V}$, $C_0 = 370 \text{ pF}$, $\alpha = 0.21 \text{ V}^{-1}$, $\beta = 0.0197 \text{ V}^{-2}$, and $C_S = 50 \text{ pF}$.

Applying the Kirchhoff laws on the network of Fig. 1 leads to the following equations that describe the propagation of waves [voltage $V_n(t)$] in the network:

$$\begin{aligned} \frac{d^2 V_n}{dt^2} + u_0^2(2V_n - V_{n+1} - V_{n-1}) + \omega_0^2 V_n + \frac{G}{C_0} \frac{dV_n}{dt} \\ + \lambda \frac{d^2}{dt^2}(2V_n - V_{n+1} - V_{n-1}) = \frac{d^2}{dt^2}(\alpha V_n^2 - \beta V_n^3), \quad (2) \end{aligned}$$

where $n = 1, 2, \dots, N$ (N being the number of cells considered), $u_0 = 1/\sqrt{L_1 C_0}$, and $\omega_0 = 1/\sqrt{L_2 C_0}$ are the characteristic frequencies of the network, $\lambda = C_S/C_0$. When using Eq. (2) to experience the transmission of solitons through the model shown in Fig. 1, one generally excites the left extremity of the line and chooses the total number of cells of the line, N , so as not to encounter the wave reflection at the end of the network.

III. MODULATED WAVES AND THE DISSIPATIVE NONLINEAR SCHRÖDINGER EQUATION

In this section, we aim to derive the amplitude equation describing the motion of modulated waves in the network of Fig. 1. We thus focus on waves with a slowly varying envelope in time and space with regard to a given carrier wave with angular frequency $\omega = \omega_p = 2\pi f$ and wave number $k = k_p$. In order to apply the reductive perturbation method [14], we introduce through the perturbative small parameter ϵ the slow envelope variables $x = \epsilon(n - v_g t)$ and $\tau = \epsilon^2 t$, and n is the cell number; here v_g designates the group velocity of the linear wave packets. Thus, the signal voltage V_n will depend explicitly not only on n and t , but also on x and τ , to separate in a natural way its fast and slow variations, in both space and time; that is $V_n(t) = V(n, t; x, \tau)$. Following Yemélé *et al.* [27,28], the solution of Eq. (2) is assumed to have the following general form:

$$\begin{aligned} V_n(t) = \epsilon A(x, \tau) \exp[i\theta] + \epsilon^2 \{B_0(x, \tau) \\ + B(x, \tau) \exp[2i\theta]\} + \text{c.c.}, \quad (3) \end{aligned}$$

where $\theta = kn - \omega t$ is the rapidly varying phase, and c.c. stands for the complex conjugate. The dc and second-harmonic terms, respectively $B_0(x, \tau)$ and $B(x, \tau)$, are added to the fundamental one $A(x, \tau)$ in order to take into account the asymmetry of the charge-voltage relation given by Eq. (1). In spite of the band-pass character of our filter, we will consider the solution (3) in its complete form, which may help in appreciating the contribution of the dc term. We then order the damping coefficient in Eq. (2) so that the damping and nonlinearity effects appear in the same perturbation equations. Thus, we set $G/C_0 = 2u_0\epsilon^2\sigma$. Substituting Eq. (3) into Eq. (2) yields a series of inhomogeneous equations at different orders of $[\epsilon, \exp[i\theta]]$. Order $[\epsilon, \exp[i\theta]]$ is associated with the linear approximation ($V_n \ll 1$) and leads to linear dispersion relation of a typical pass band filter

$$\omega^2 = \frac{\omega_0^2 + 4u_0^2 \sin^2 \frac{k}{2}}{1 + 4\lambda \sin^2 \frac{k}{2}}. \quad (4)$$

The corresponding linear group velocity is

$$v_g = \frac{d\omega}{dk} = \frac{(u_0^2 - \lambda\omega_0^2) \sin k}{\omega(1 + 4\lambda \sin^2 \frac{k}{2})^2}. \quad (5)$$

To order $[\epsilon^3, \exp[i\theta]]$ we get the dissipative nonlinear Schrödinger equation governing the slow envelope evolution

$$i \frac{\partial A}{\partial \tau} + P \frac{\partial^2 A}{\partial x^2} + Q|A|^2 A + i\Gamma A = 0, \quad (6)$$

where

$$P = \frac{[u_0^2 + \lambda(2v_g^2 - \omega^2)] \cos k - 4\lambda\omega v_g \sin k - (1 + 2\lambda)u_g^2}{2\omega(1 + 4\lambda \sin^2 \frac{k}{2})}, \quad (7a)$$

$$\begin{aligned} Q = \frac{3\beta\omega}{2(1 + 4\lambda \sin^2 \frac{k}{2})} - \frac{4v_g^2\alpha^2\omega}{(v_g^2 - u_0^2)(1 + 4\lambda \sin^2 \frac{k}{2})} \\ - \frac{\alpha^2\omega^3}{(1 + 4\lambda \sin^2 \frac{k}{2})[\omega^2 + (4\lambda\omega^2 - u_0^2) \sin^2 k - \frac{\omega_0^2}{4}]}, \quad (7b) \end{aligned}$$

$$\Gamma = \frac{u_0\sigma}{(1 + 4\lambda \sin^2 \frac{k}{2})}, \quad (7c)$$

respectively, represent the dispersion, the nonlinearity, and the dissipation. A similar solution to the nonlinear Schrödinger equation (6) has already been derived by Marquié *et al.* [29] when studying the modulational instability in a real electrical lattice and has been used by Giannini *et al.* [30] to investigate the propagation of bright and dark solitons in lossy optical fibers.

To orders $[\epsilon^2, \exp[2i\theta]]$ and $[\epsilon^4, \exp[0i\theta]]$, we respectively obtain the second harmonic and the continuous components B and B_0 of the voltage:

$$\begin{aligned} B(x, \tau) = \frac{\alpha\omega^2}{\omega^2 + (4\omega^2\lambda - u_0^2) \sin^2 k - \frac{\omega_0^2}{4}} A^2, \\ B_0(x, \tau) = \frac{2\alpha v_g^2}{v_g^2 - u_0^2} |A|^2. \quad (8) \end{aligned}$$

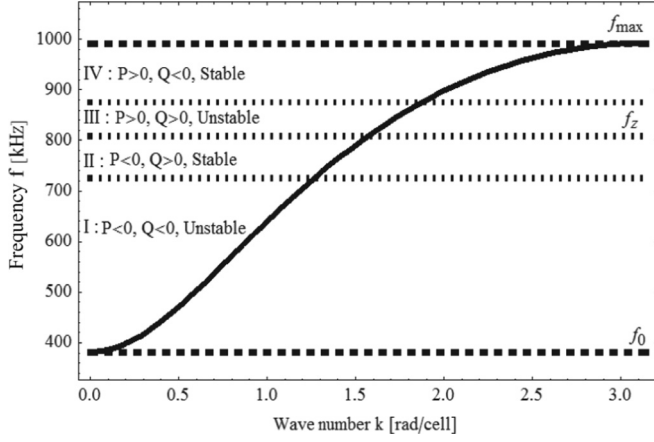


FIG. 2. Linear dispersive curve of the network showing evolution of the frequency $f = \omega/2\pi$ as function of the wave number k for the network parameters $L_1 = 200 \mu\text{H}$, $L_2 = 470 \mu\text{H}$, $V_b = 2 \text{V}$, $C_0 = 370 \text{pF}$, $\alpha = 0.21 \text{V}^{-1}$, $\beta = 0.0197 \text{V}^{-2}$, and $C_S = 50 \text{pF}$. The lower cutoff frequency is $f_0 = 381.65 \text{kHz}$ (dashed line), and the upper cutoff frequency is $f_{\max} = 991.63 \text{kHz}$ (dash-dotted line).

Comparing Eq. (7b) with Eq. (8), we conclude that the second and third terms of the nonlinearity coefficient Q come from the contribution of $B_0(x, \tau)$ and $B(x, \tau)$, respectively. It is seen from Eq. (7c) that the dissipative coefficient Γ is due to the dissipative element G of the network and increases with the dissipative parameter σ . As we can see from Eqs. (7a), (7b), and (7c), the dispersion coefficient P , the nonlinear coefficient Q , and the dissipative coefficient Γ are all functions of the wave number k . For values of k chosen in the first Brillouin zone ($0 \leq k \leq \pi$), we plot in Fig. 2 P , Q , and product $P \times Q$ as functions of wave number k for the above network parameters. As we can see from the dispersion curve [Fig. 2(a)], the dispersion coefficient P vanishes for the value of the wave number $k_z \simeq 1.5708 \text{ rad/cell}$ that corresponds to the frequency $f_z \simeq 808.46 \text{ kHz}$. Figure 2(b) shows that for the above network coefficients, the nonlinear coefficient Q is negative for almost all wave number k from the first Brillouin zone, except for $k \in [k_1, k_2]$ where $k_1 \simeq 1.2677 \text{ rad/cell}$ and $k_2 \simeq 1.87389 \text{ rad/cell}$ corresponding to frequencies $f_1 = \omega(k_1)/(2\pi) \simeq 725.372 \text{ kHz}$ and $f_2 = \omega(k_2)/(2\pi) \simeq 875.121 \text{ kHz}$, respectively. Therefore, product PQ is positive for $k \in [0, k_1] \cup [k_2, \pi]$ and negative for $k \in]k_1, k_2[$ [this can be seen from Fig. 2(c)]. In summary, we have four different regions concerning the modulational instability of a plane wave and the possible soliton solutions:

1. Region I: $f \in [f_0, \omega(k_1)/2\pi]$, i.e., $f \in [381.654, 725.372]$, $PQ > 0 \Rightarrow \text{Unstable} \Rightarrow \text{Bright Solitons}$

2. Region II: $f \in [\omega(k_1)/2\pi, f_z]$, i.e., $f \in [725.372, 808.46]$,

$PQ < 0 \Rightarrow \text{Stable} \Rightarrow \text{Dark Solitons}$

3. Region III: $f \in [f_z, \omega(k_2)/2\pi]$, i.e., $f \in [808.46, 875.121]$,

$PQ > 0 \Rightarrow \text{Unstable} \Rightarrow \text{Bright Solitons}$

4. Region IV: $f \in [\omega(k_2)/2\pi, f_{\max}]$, i.e., $f \in [875.121, 991.632]$,

$PQ < 0 \Rightarrow \text{Stable} \Rightarrow \text{Dark Solitons}$. Here $f_0 = \omega_0/2\pi$ and $f_{\max} = \omega_{\max} = (2\pi)^{-1} \sqrt{\omega_0^2 + 4u_0^2}/(1 + 4\lambda)$. Note that for

$P = 0$, $f = f_z = \omega(k_z)/2\pi$. Figure 2 shows the linear dispersion curve associated with Eq. (4) and different regions of the MI for the above network parameters.

IV. EXACT BRIGHT, DARK, AND KINK SOLITARY WAVELIKE SOLUTIONS OF THE DISSIPATIVE NLS EQUATION OF THE NETWORK

We start this section by noting that the partition of the bandwidth is not a real problem. The important point is only that some frequency regions correspond to positive PQ leading to envelope solitons, whereas another ones correspond to negative PQ leading to hole and kink solitons. The variation of the sign of product PQ piques our interest in the analytical study of envelope, hole, and kink solitons in our network.

In this section, we find exact solitary wavelike solutions of the dissipative NLS equation (6). It is well known that in the absence of the dissipative term, i.e., $\Gamma = 0$, Eq. (6) admits both bright and dark soliton solutions. Equation (6) is not longer integrable if its dissipative term Γ is not zero; in this section, we attempt to find its analytical solitary wavelike solutions when $\Gamma \neq 0$. For this purpose, we introduce ansatz

$$A(x, \tau) = a(\tau)u(X) \exp\{i[Kx - \varphi(\tau)]\}, \quad (9)$$

$$X = X(x, \tau) = \alpha_0(\tau)x + \beta_0(\tau),$$

where K is a real constant, $a(\tau)$, $\alpha_0(\tau)$, $\beta_0(\tau)$, and $\varphi(\tau)$ are a real function of variable τ to be determined, and u is a real function of variable X . Inserting ansatz (9) into Eq. (6) and separating real and imaginary parts yield

$$P\alpha_0^2 \left(\frac{du}{dX} \right)^2 + 2Qa^2u^4 + \left[\frac{d\varphi(\tau)}{d\tau} - PK^2 \right] u^2 - A_0 = 0, \quad (10a)$$

$$\left(\frac{da}{d\tau} + \Gamma \right) u + \left(\frac{d\beta_0}{d\tau} - \frac{1}{\alpha_0} \frac{d\alpha_0}{d\tau} \beta_0 + 2PK\alpha_0 + \frac{\frac{d\alpha_0}{d\tau}}{\alpha_0} X \right) \frac{du}{dX} = 0, \quad (10b)$$

where $A_0(\tau)$ is an arbitrary function of τ (constant of integration with respect with X). Demanding that α_0 and β_0 satisfy equation

$$\frac{d\beta_0}{d\tau} - \frac{1}{\alpha_0} \frac{d\alpha_0}{d\tau} \beta_0(\tau) + 2PK\alpha_0 = 0$$

yields

$$\beta_0(\tau) = -2PK\tau\alpha_0(\tau) + K_0\alpha_0(\tau), \quad (11)$$

$$X = \alpha_0(\tau)[x - 2PK\tau + K_0],$$

where K_0 is an arbitrary real parameter. Inserting Eq. (11) into system (10a)–(10b) yields

$$P\alpha_0^2(\tau) \left(\frac{du}{dX} \right)^2 + 2Qa^2u^4 + \left[\frac{d\varphi(\tau)}{d\tau} - PK^2 \right] u^2 - A_0 = 0, \quad (12a)$$

$$\left(\frac{1}{a} \frac{da}{d\tau} + \Gamma \right) u + \left(\frac{X}{\alpha_0} \frac{d\alpha_0}{d\tau} \right) \frac{du}{dX} = 0. \quad (12b)$$

Equation 12(a) is an elliptic ordinary differential equation (EODE). The simplest functions $\alpha_0(\tau)$ and $a(\tau)$ for which

Eq. 12(b) is satisfied for every $u(X)$ are obtained by asking that the coefficients of u and du/dX in this equation vanish, i.e., $\frac{1}{a} \frac{da}{d\tau} + \Gamma = 0$ and $\frac{X}{\alpha_0} \frac{d\alpha_0}{d\tau} = 0$. This leads to

$$a(\tau) = a_0 \exp[-\Gamma\tau], \quad \alpha_0(\tau) = \alpha_{00}, \quad (13)$$

where $a_0 \neq 0$ and $\alpha_{00} \neq 0$ are two real constants. Thus, if $a(\tau)$ and $\alpha_0(\tau)$ are defined by Eq. (13), system (12a)–(12b) becomes

$$\left(\frac{du}{dX}\right)^2 = -\frac{2Qa^2}{P\alpha_0^2}u^4 + \frac{PK^2 - \frac{d\varphi}{d\tau}}{P\alpha_0^2}u^2 + \frac{A_0}{P\alpha_0^2}, \quad (14)$$

that we rewrite in the form

$$\left(\frac{d\rho}{dX}\right)^2 = -\frac{8Qa^2}{6P\alpha_0^2}\rho^3 + \frac{4[PK^2 - \frac{d\varphi(\tau)}{d\tau}]}{P\alpha_0^2}\rho^2 + 4\frac{A_0}{P\alpha_0^2}\rho, \quad (15)$$

$$u^2 = \rho.$$

Equations (14) and (15) are EODEs. Each of these two equations is a special case of the equation

$$\left(\frac{dy}{dX}\right)^2 = \alpha_1 y^4 + 4\beta_1 y^3 + 6\gamma_1 y^2 + 4\delta_1 y + \varepsilon_1 \stackrel{\text{def.}}{=} \Lambda(y), \quad (16)$$

where $\alpha_1, \beta_1, \gamma_1, \delta_1,$ and ε_1 are functions of variable τ defined as

$$\alpha_1 = \begin{cases} -\frac{2Qa^2}{P\alpha_0^2} & \text{for Eq. (14),} \\ 0 & \text{for Eq. (15);} \end{cases} \quad \beta_1 = \begin{cases} 0 & \text{for Eq. (14),} \\ -\frac{4Qa^2}{3P\alpha_0^2} & \text{for Eq. (15);} \end{cases}$$

$$\gamma_1 = \begin{cases} \frac{2(PK^2 - \frac{d\varphi(\tau)}{d\tau})}{3P\alpha_0^2} & \text{for Eq. (14),} \\ 0 & \text{for Eq. (15);} \end{cases}$$

$$\delta_1 = \begin{cases} 0 & \text{for Eq. (14),} \\ \frac{A_0}{P\alpha_0^2} & \text{for Eq. (15);} \end{cases} \quad \varepsilon_1 = \begin{cases} \frac{A_0}{P\alpha_0^2} & \text{for Eq. (14),} \\ 0 & \text{for Eq. (15).} \end{cases}$$

In some special cases, we can express solitary wavelike solutions of Eq. (16) in terms of $P, Q, \alpha_0, a, \varphi, K,$ and A_0 . In our analysis, we mainly use Eq. (14) [Eq. (15) will be used only occasionally].

To find analytical solitary wavelike solutions of Eq. (16) in explicit form, we use either the direct method or the Weierstrass’s elliptic function method [31,32]. It is well known that a large class of solutions of Eq. (16) is given by expression [31,32]

$$y(X) = y_0 + \frac{\sqrt{\Lambda(y_0)} \frac{d\varphi(X; g_2, g_3)}{dX} + \frac{1}{2} \Lambda'(y_0) [\wp(X; g_2, g_3) - \frac{1}{24} \Lambda''(y_0)] + \frac{1}{24} h(y_0) \Lambda'''(y_0)}{2[\wp(X; g_2, g_3) - \frac{1}{24} \Lambda''(y_0)]^2 - \frac{1}{48} \Lambda(y_0) \Lambda'''(y_0)}, \quad (17)$$

where y_0 is any real function of τ [not necessary a root of polynomial $\Lambda(y)$] and $\wp(X; g_2, g_3)$ is the Weierstrass’s elliptic function with invariants $g_2 = \alpha_1 \varepsilon_1 - 4\beta_1 \delta_1 + 3\gamma_1^2$ and $g_3 = \alpha_1 \gamma_1 \varepsilon_1 + 2\beta_1 \gamma_1 \delta - \alpha \delta^2 - \gamma^3 - \varepsilon_1 \beta_1$. Equation (17) leads to solitary wavelike solutions of Eq. (16) only when the following three conditions are satisfied simultaneously [33]:

$$\Delta = g_2^3 - 27g_3^2 = 0, \quad g_2 \geq 0, \quad g_3 \leq 0. \quad (18)$$

When y_0 is a simple root of polynomial $\Lambda(y)$, Eq. (17) leads to the solitary wavelike solution having the form [33]

$$y(X) = y_0 + \frac{\Lambda'(y_0)}{4\{e_1 - \frac{\Lambda''(y_0)}{24} + 3e_1 \cosh^2[\sqrt{3}e_1 X]\}}, \quad (19)$$

$$e_1 = \frac{1}{2} \sqrt[3]{-g_3}.$$

It is important to note that expression (19) is used for the solitary wavelike solution of Eq. (16) only if y_0 is a simple root of polynomial $\Lambda(y)$.

We notice that any solitary wavelike solution of the EOD equation (16) leading to a solitary wavelike solution $u(X)$ of Eq. (14) gives the following solitary wavelike solution of the dissipative NLS Eq. (6):

$$A(x, \tau) = a_0 \exp[-\Gamma\tau] u(\alpha_{00}[x - 2PK\tau + K_0]) \times \exp\{i[Kx - \varphi(\tau)]\}. \quad (20)$$

In what follows, we distinguish the case of bright and dark and kink solitary wavelike solutions.

A. Analytical bright solitary wavelike solutions of the OEDE

As we have mentioned above, solitary wavelike solutions of Eq. (14) will be sought either by the direct method or the Weierstrass’s elliptic function method.

1. Direct method for exact bright soliton solutions to the OEDE

As examples of the use of the direct method, we seek soliton solutions of Eq. (14) having either the form $u(X) = 1/\cosh[mX]$ or $u(X) = 1/(A_1 + B_1 \cosh^2[mX])$. Imposing to $u(X)$ to satisfy Eq. (14) yields

$$u(X) = \frac{1}{\cosh\left[\frac{a}{\alpha_0} \sqrt{\frac{2Q}{P}} X\right]},$$

$$\varphi(\tau) = \begin{cases} (K^2 P - 2Q\alpha_0^2)\tau - \varphi_0, & \text{if } \Gamma = 0 \\ K^2 P\tau + \frac{Q\alpha_0^2}{\Gamma} \exp[-2\Gamma\tau] - \varphi_0, & \text{if } \Gamma \neq 0 \end{cases} \quad (21a)$$

$$u(X) = \pm \frac{1}{a} \sqrt{\frac{PK^2 - \frac{d\varphi(\tau)}{d\tau}}{2Q}} \frac{1}{1 - 2 \cosh^2\left[\frac{1}{2\alpha_0} \sqrt{\frac{PK^2 - \frac{d\varphi(\tau)}{d\tau}}{P}} X\right]}, \quad (21b)$$

respectively. In solution 21(b), $\varphi(\tau)$ is an arbitrary function that satisfies conditions $P[PK^2 - \frac{d\varphi(\tau)}{d\tau}] > 0$ and $Q[PK^2 - \frac{d\varphi(\tau)}{d\tau}] > 0$. Both Eqs. 21(a) and 21(b) give soliton

solutions of Eq. (14) with vanishing boundary conditions $u(\pm\infty) = 0$.

2. Weierstrass's elliptic function method for exact solitary wavelike solutions to the OEDE

Now we apply Weierstrass's elliptic function method to find exact bright solitary wavelike solutions of either Eq. (14) or (15). We start with Eq. (14). For Eq. (14), conditions (18) for solitary wavelike solutions read

$$\begin{aligned} A_0 \left\{ 8A_0 Q a^2 + \left[PK^2 - \frac{d\varphi(\tau)}{d\tau} \right]^2 \right\} &= 0, \\ \left[PK^2 - \frac{d\varphi(\tau)}{d\tau} \right]^2 - 24A_0 Q a^2 &\geq 0, \\ P \left[PK^2 - \frac{d\varphi(\tau)}{d\tau} \right] \left\{ 72A_0 Q a^2 + \left[PK^2 - \frac{d\varphi(\tau)}{d\tau} \right]^2 \right\} &\geq 0. \end{aligned} \tag{22}$$

If $A_0 = 0$, the first two conditions are satisfied, while the last one is satisfied only if $P[PK^2 - \frac{d\varphi(\tau)}{d\tau}] \geq 0$. In this case, polynomial Λ admits two simple roots, namely, $u_0 = \pm\sqrt{\frac{PK^2 - \frac{d\varphi}{d\tau}}{2Qa^2}}$ if and only if $Q[PK^2 - \frac{d\varphi(\tau)}{d\tau}] > 0$. Using expression (19) for each of these simple roots yields

$$\begin{aligned} u(X) &= \pm \frac{1}{a} \sqrt{\frac{PK^2 - \frac{d\varphi(\tau)}{d\tau}}{2Q}} \\ &\times \left\{ 1 - \frac{12}{1 + 6 \cosh^2 \left[\frac{1}{2\alpha_0} \sqrt{P^{-1} \left(PK^2 - \frac{d\varphi}{d\tau} \right) X} \right]} \right\}. \end{aligned} \tag{23}$$

It is obvious that (23) is a solitary wavelike solution of Eq. (14) with nonvanishing boundary conditions.

If $A_0 \neq 0$, the first of conditions (22) for solitary wavelike solutions of Eq. (14) yields $A_0 = -\frac{1}{8Qa^2} [PK^2 - \frac{d\varphi(\tau)}{d\tau}]^2$, leading to $\Lambda(u) = -\frac{2Qa^2}{P\alpha_0^2} (u^2 - \frac{PK^2 - \frac{d\varphi}{d\tau}}{4Qa^2})^2$. Evaluating e_1 in this case yields $e_1 = -\frac{[PK^2 - \frac{d\varphi(\tau)}{d\tau}]}{6P\alpha_0^2}$. It follows from the expression for $\Lambda(u)$ that polynomial $\Lambda(u)$ does not have any simple root.

B. Analytical expression for dark (kink) soliton solutions of the OEDE

We now apply direct method and Weierstrass's elliptic function method to find analytical dark soliton solutions $u(X)$ of Eq. (14).

1. Direct method for exact dark solutions to the OEDE

Here we find an exact dark soliton solution of Eq. (14) by substituting $u(X) = \tanh [mX]$ in Eq. (14). As the result, we obtain the dark soliton solution

$$\begin{aligned} u(X) &= \tanh \left[\frac{a}{\alpha_0} \sqrt{-\frac{2Q}{P}} X \right], \\ \varphi(\tau) &= K^2 P \tau - \frac{2Qa_0^2}{\Gamma} \exp[-2\Gamma\tau] - \varphi_0, \end{aligned} \tag{24}$$

where φ_0 is an arbitrary real constant.

2. Weierstrass's elliptic function method for exact dark and/or kink soliton solutions to the OEDE

Now we apply the Weierstrass's elliptic function method to find dark and/or kink soliton solutions of Eq. (14). These solutions are associated with nonzero multiple roots of polynomial Λ for Eq. (14) and/or Eq. (15) [33]. For a multiple root of polynomial Λ , we use Eq. (17) instead of Eq. (19) to evaluate the corresponding soliton solutions.

We start with Eq. (14). When $A_0 \neq 0$, we found, under the conditions of solitary wavelike solutions (22), that polynomial Λ for Eq. (14) admits two double roots $u_0 = \pm\frac{1}{2}\sqrt{\frac{PK^2 - \frac{d\varphi}{d\tau}}{Qa^2}}$, if $\varphi(\tau)$ is chosen from condition $Q(PK^2 - \frac{d\varphi}{d\tau}) > 0$. Let us, as an example, consider the double root $u_0 = \frac{1}{2}\sqrt{\frac{PK^2 - \frac{d\varphi}{d\tau}}{Qa^2}}$. Noting that $e_1 = -\frac{PK^2 - \frac{d\varphi(\tau)}{d\tau}}{6P\alpha_0^2}$ and choosing $u_0 = \frac{1}{4a}\sqrt{\frac{PK^2 - \frac{d\varphi(\tau)}{d\tau}}{Q}}$ [33], Eq. (17) for $\wp = e_1 + \frac{3e_1}{\sinh^2(\sqrt{3}e_1 X)}$ gives the kink soliton solution

$$u(X) = \frac{1}{2a} \sqrt{\frac{PK^2 - \frac{d\varphi(\tau)}{d\tau}}{Q}} \frac{\left\{ 4 + 3 \sinh \left[\frac{2}{\alpha_0} \sqrt{-\frac{PK^2 - \frac{d\varphi(\tau)}{d\tau}}{2P}} X \right] \right\}}{5 + 3 \cosh \left[\frac{2}{\alpha_0} \sqrt{-\frac{PK^2 - \frac{d\varphi(\tau)}{d\tau}}{2P}} X \right]}, \tag{25}$$

where $Q(PK^2 - \frac{d\varphi}{d\tau}) > 0$ and, consequently, $P(PK^2 - \frac{d\varphi}{d\tau}) < 0$.

We now use Eq. (15) to generate another dark soliton solution of Eq. (14). For this equation, conditions (18) for soliton solutions give $8Qa^2 A_0 + [\frac{d\varphi(\tau)}{d\tau} - PK^2]^2 = 0$ and $P[PK^2 - \frac{d\varphi(\tau)}{d\tau}] \leq 0$. Solving the first equation in A_0 and inserting the result in $\Lambda(\rho)$ yield $\Lambda(\rho) = -\frac{8Qa^2}{P\alpha_0^2} \rho \left[\rho - \frac{PK^2 - \frac{d\varphi(\tau)}{d\tau}}{4Qa^2} \right]^2$. Therefore, $\Lambda(\rho)$ admits one double root, $\rho_0 = \frac{PK^2 - \frac{d\varphi(\tau)}{d\tau}}{4Qa^2}$. Noting that $e_1 = -\frac{PK^2 - \frac{d\varphi(\tau)}{d\tau}}{6P\alpha_0^2}$ and choosing $\rho_0 = \frac{PK^2 - \frac{d\varphi(\tau)}{d\tau}}{8Qa^2}$ [33], we evaluate Eq. (17) for $\wp = e_1 + \frac{3e_1}{\sinh^2(\sqrt{3}e_1 X)}$ and use the relationship $u^2 = \rho$ to get the following dark soliton solution:

$$u(X) = \pm \frac{1}{2a} \sqrt{\frac{PK^2 - \frac{d\varphi(\tau)}{d\tau}}{Q}} \frac{\sqrt{2 + \sinh^2(\sqrt{3}e_1 X) + \sinh^4(\sqrt{3}e_1 X) - 2 \cosh(\sqrt{3}e_1 X) \sinh(\sqrt{3}e_1 X)}}{2 + \sinh^2(\sqrt{3}e_1 X)}. \tag{26}$$

Here $e_1 = -\frac{PK^2 - \frac{d\varphi(\tau)}{d\tau}}{6P\alpha_0^2}$. Note that under condition $P[PK^2 - \frac{d\varphi(\tau)}{d\tau}] < 0$, we automatically have $Q[PK^2 - \frac{d\varphi(\tau)}{d\tau}] > 0$ since $PQ < 0$.

V. PROPAGATION OF BRIGHT, DARK, AND KINK SOLITARY WAVELIKE THROUGH THE NETWORK OF FIG. 1

In this section we use the exact solutions of the dissipative NLS equation (6) to investigate analytically the propagation of bright, dark, and kink solitary wavelike through the network of Fig. 1. We focus on the case of $\Gamma \neq 0$.

A. Propagation of bright solitary waves in the network of Fig. 1

Each of the bright soliton solutions 21(a) and 21(b) and the solitary wavelike solution (23) of the EODE (14)

$$A(x, \tau) = \frac{a_0 \exp[-\Gamma\tau] \exp \left\{ i \left(Kx - K^2 P\tau - \frac{Qa_0^2}{\Gamma} \exp[-2\Gamma\tau] + \varphi_0 \right) \right\}}{\cosh \left\{ a_0 \sqrt{\frac{2Q}{P}} \exp[-\Gamma\tau] [x - 2PK\tau + K_0] \right\}}, \quad \Gamma \neq 0, \quad (27a)$$

$$A(x, \tau) = \frac{a_0 \exp \left\{ i \left(Kx - [K^2 P - 2Qa_0^2] \tau + \varphi_0 \right) \right\}}{\cosh \left\{ a_0 \sqrt{\frac{2Q}{P}} (x - 2PK\tau + K_0) \right\}}, \quad \Gamma \neq 0. \quad (27b)$$

It is seen from Eq. 27(a) that the soliton amplitude a_0 is proportional to function $\exp[-\Gamma\tau]$, while its width is inversely proportional to function $\sqrt{\frac{2Q}{P}} \exp[-\Gamma\tau]$. Because Γ is a positive parameter, function $\exp[-\Gamma\tau]$ decreases when Γ increases (we remember that $\tau = \epsilon^2 t > 0$). In other words, the soliton width increases when the dissipative element G of the network increases. Meantime, the soliton amplitude decreases when the dissipative element of the network increases. The center of bright soliton is $\xi(\tau) = \sqrt{\frac{P}{2Q}} (2PK\tau + K_0) \exp[\Gamma\tau]$, and satisfies equation $\frac{d^2 \xi(\tau)}{d\tau^2} - \frac{\Gamma[4PK + \Gamma(2PK\tau + K_0)]}{2PK\tau + K_0} \xi(\tau) = 0$. This equation means that the center of mass of the macroscopic wave packet behaves like a classical particle and allows us to manipulate the motion of bright soliton in the network by controlling the dissipative element G .

Figure 3 shows the propagation of solitary signal at frequency $f = 406.881\text{kHz}$ for the above network parameters and solution parameters $a_0 = 50$, $\varphi_0 = -20$, $K = -0.1$, and $\epsilon = 10^{-3}$. It is seen from Figs. 3(a) and 3(c) that the cell number n does not affect either the peak value of wave amplitude or the wave width. Figure 3(b) shows that the wave amplitude decreases while the wave width increases when the dissipative parameter σ increases.

Now we consider the solitary wavelike solution (23) of the EODE (14). This solution of the EODE (14) leads to the following bright solitary wavelike solution of the dissipative NLS equation (6)

$$\begin{aligned} A(x, \tau) &= \pm \sqrt{\frac{PK^2 - \frac{d\varphi(\tau)}{d\tau}}{2Q}} \\ &\times \left(1 - \frac{12}{1 + 6 \cosh^2 \left[\frac{1}{2} \sqrt{\frac{PK^2 - \frac{d\varphi}{d\tau}}{P}} (x - 2PK\tau + K_0) \right]} \right) \\ &\times \exp[i(Kx - \varphi(\tau))], \end{aligned} \quad (28)$$

leads, respectively, to bright soliton solutions and a bright solitary wavelike solution of Eq. (6) and consequently, to the propagation of bright solitons and bright solitary waves in the network of Fig. 1. It is important to notice that each of solutions 21(b) and (23) of the EODE (14) contains the free functional parameter $\varphi(\tau)$, which will be chosen under some conditions on P and/or Q . This free functional parameter will allow us to manipulate the motion of the solitary waves on the network. We will limit ourselves to the use of solutions 21(a) and (23) [one solution without the free parameter $\varphi(\tau)$ and one solution that contains $\varphi(\tau)$].

We start with the solution 21(a) that we write the corresponding solution of Eq. (6) as follows:

where the functional parameter $\varphi(\tau)$ and constant K are to be taken from conditions $P[PK^2 - \frac{d\varphi(\tau)}{d\tau}] > 0$ and $Q[PK^2 - \frac{d\varphi(\tau)}{d\tau}] > 0$. Although if the solitary wavelike solution (28) of the dissipative NLS equation (6) does not contain (explicitly) the dissipative coefficient Γ , parameters K and $\varphi(\tau)$ appearing in this solution result from the existence of the dissipative term in Eq. (6).

For the above network parameters and a given set of solution parameters, we show in Fig. 4 the propagation of bright solitary waves through cell $n = 25$ of the network for different expressions for $d\varphi(\tau)/d\tau$. This figure shows how we can manage the bright solitary waves motion in the line just by manipulating the functional parameter $\varphi(\tau)$.

B. Propagation of kink solitons in the network of Fig. 1

Based on an exact kink soliton solution of Eq. (14), we investigate analytically the propagation of kink solitons in the network of Fig. 1. The kink soliton solution (24) of the EODE (14) is associated with the following kink soliton solution of the dissipative NLS equation (6):

$$\begin{aligned} A(x, \tau) &= a_0 \exp[-\Gamma\tau] \tanh \\ &\times \left\{ a_0 \sqrt{-\frac{2Q}{P}} \exp[-\Gamma\tau] [x - 2PK\tau + K_0] \right\} \\ &\times \exp \left\{ i \left(Kx - K^2 P\tau + \frac{2Qa_0^2}{\Gamma} \exp[-2\Gamma\tau] + \varphi_0 \right) \right\}. \end{aligned} \quad (29)$$

It is seen from solution (29) that the wave amplitude a_0 is proportional to the function $\exp[-\Gamma\tau]$ while its width is inversely proportional to $\sqrt{-\frac{2Q}{P}} \exp[-\Gamma\tau]$. Therefore, solution (29) can be used to describe the compression of kink solitons of the network of Fig. 1. With the help of the exact kink soliton solution (29) of the dissipative NLS equation (6),

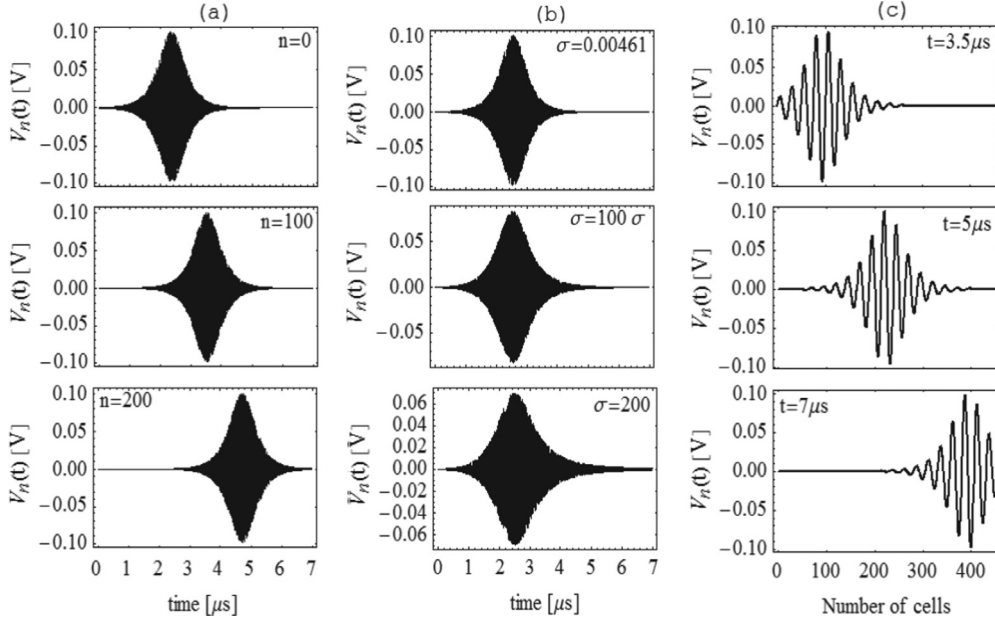


FIG. 3. Signal voltage obtained with the exact bright soliton solution 27(a) of the dissipative NLS equation (6) for the network parameters shown in the text and for frequency $f = 406.881$ kHz. (a) Propagation of bright soliton signal at different cells of the network. (b) Propagation of bright soliton signal at cell $n = 15$ of the network for different dissipative parameter σ . (c) Spatial propagation of bright soliton through the network at different times for $\sigma = 0.00461$.

we show in Fig. 5 the dynamics of kink solitons propagating through the network for the above line parameters. Plots of Figs. 5(a) and 5(c) show that the wave amplitude does not vary with the cell number n . Plots of Fig. 5(b) show that the wave amplitude decreases while its width increases when the dissipative parameter σ increases. For a better understanding, we show in Fig. 6 the time evolution of kink solitons through

cell $n = 15$ at frequency $f = 777.275$ kHz for three different values of the dissipative parameter σ .

C. Propagation of dark solitons in the network of Fig. 1

We end this section with the analytical investigation of the dynamics of dark solitons propagating through the network.

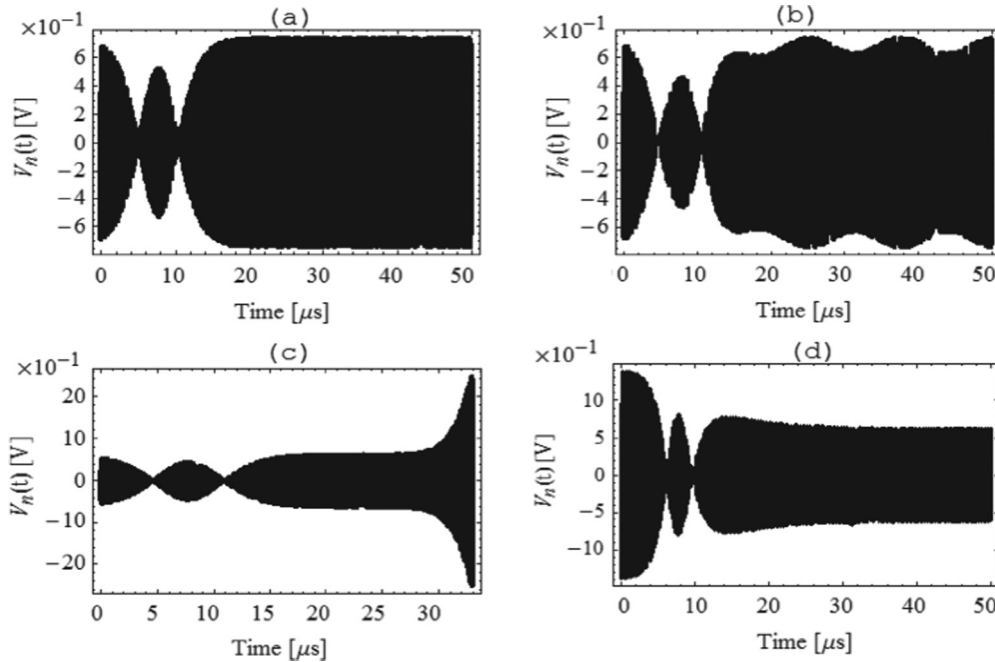


FIG. 4. Propagation of bright solitary waves in the network at frequency $f = 849.872$ kHz obtained with the exact bright solitary wavelike solution (28) of the dissipative NLS equation (6) for the network parameters shown in the text and the solution parameters $\epsilon = 10^{-2}$, $K = 0.1$, $K_0 = 40$ and (a) $\frac{d\varphi(\tau)}{d\tau} = -10^0$; (b) $\frac{d\varphi(\tau)}{d\tau} = -10^9 \cos^2 [250\,000\epsilon^{-2}\tau]$; (c) $\frac{d\varphi}{d\tau} = -2 \times 10^{-4} \exp [10^6\epsilon^{-2}\tau]$; (d) $\frac{d\varphi}{d\tau} = -10^{10} \cosh^{-2} [10^5\epsilon^{-2}\tau]$.

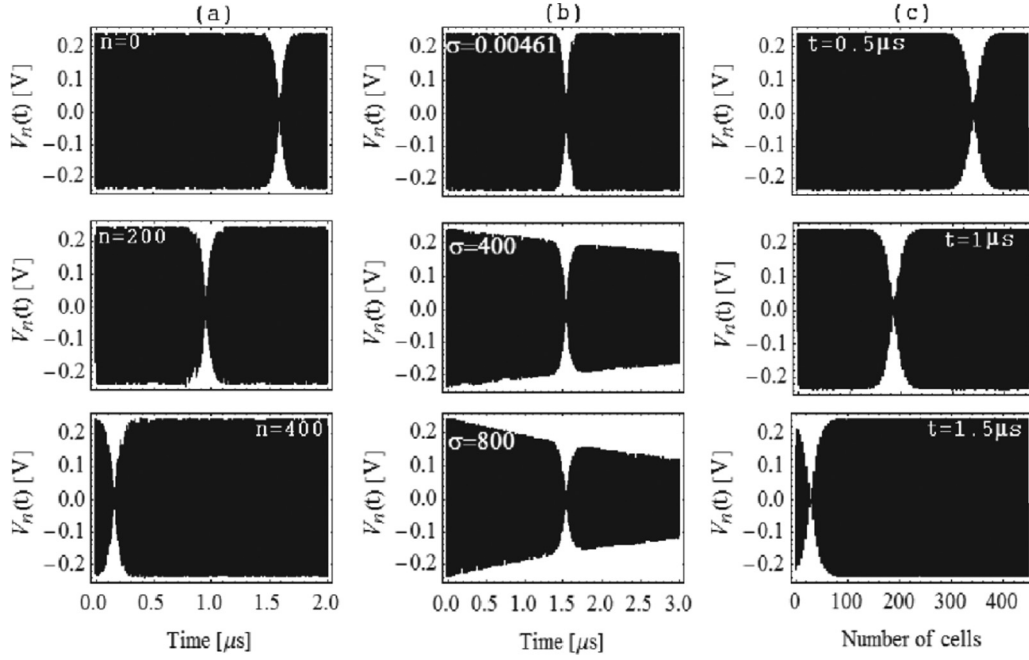


FIG. 5. Propagation of kink soliton in the network at frequency $f = 777.275$ kHz for the above line parameters and the solution parameters $a_0 = 12$, $\varphi_0 = 0.1$, $K_0 = -5$, $K = 0.1$, and $\varepsilon = 10^{-2}$. (a) Evolution of kink soliton at three different cells; (b) evolution of kink soliton at cell $n = 25$ for three values of the dissipative parameter σ ; (c) profile of the kink soliton at three different times.

For this purpose, we use the exact solution (26) of the EODE (14) which leads to the following exact dark soliton solution of the dissipative NLS equation (6):

$$\begin{aligned}
 A(x, \tau) = & \frac{\pm \sqrt{\frac{PK^2 - \frac{d\varphi(\tau)}{d\tau}}{Q}} \exp[i(Kx - \varphi(\tau))]}{2 \left\{ 2 + \sinh^2 \left[\sqrt{-\frac{PK^2 - \frac{d\varphi(\tau)}{d\tau}}{2P}} (x - 2PK\tau + K_0) \right] \right\}} \\
 & \times \left\{ 2 - \sinh \left[2 \sqrt{-\frac{PK^2 - \frac{d\varphi(\tau)}{d\tau}}{2P}} (x - 2PK\tau + K_0) \right] \right. \\
 & + \sinh^2 \left[\sqrt{-\frac{PK^2 - \frac{d\varphi(\tau)}{d\tau}}{2P}} (x - 2PK\tau + K_0) \right] \\
 & \left. + \sinh^4 \left[\sqrt{-\frac{PK^2 - \frac{d\varphi(\tau)}{d\tau}}{2P}} (x - 2PK\tau + K_0) \right] \right\}^{\frac{1}{2}}, \quad (30)
 \end{aligned}$$

where constant K and the functional parameter $\varphi(\tau)$ are to be chosen from conditions $P[PK^2 - \frac{d\varphi(\tau)}{d\tau}] < 0$ and $Q[PK^2 - \frac{d\varphi(\tau)}{d\tau}] > 0$. It is obvious that the dissipative parameter Γ does not appear explicitly in (30). Meanwhile, parameters K and K_0 and the functional parameter $\varphi(\tau)$ result from the presence of Γ in Eq. (6). For a given set of solution parameters and the above network parameters, we show in Fig. 7 the time evolution of dark soliton through cell $n = 250$ of the network for different functional parameter $\varphi(\tau)$. Plots of this figure show how we may use parameter $\varphi(\tau)$ to manipulate the motion of dark solitons through the network.

VI. CONCLUSION

In this work, we have studied the dynamics of modulated waves in a modified Noguchi electrical transmission line with dissipative elements. In the continuum limit, we have used the semidiscrete approximation to establish that the motion of modulated waves in the network is governed by a dissipative nonlinear Schrödinger equation. Based on the dissipative NLS equation and the linear dispersion law, our study predicted four frequency regions with different behaviors concerning the modulational instability of a plane wave, two regions associated with the envelope solitons which alternate with two regions for dark or kink solitons. Motivated with the solitary wave type of solutions to the classical nonlinear Schrödinger equation, we have used both the direct method and the

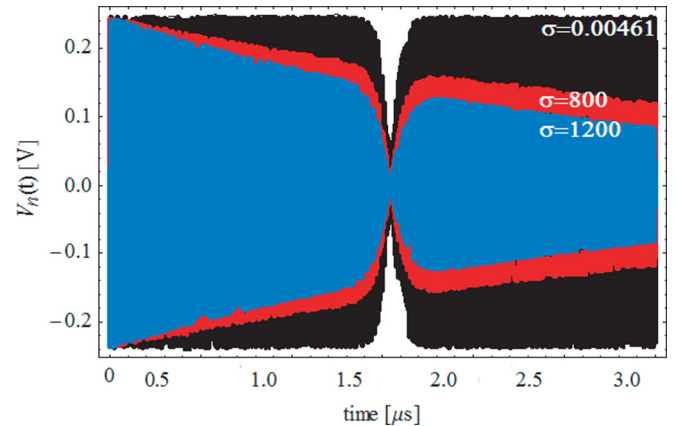


FIG. 6. (Color online) Effects of the dissipative element of the network on the kink soliton propagating through cell $n = 15$ at frequency $f = 777.275$ kHz.

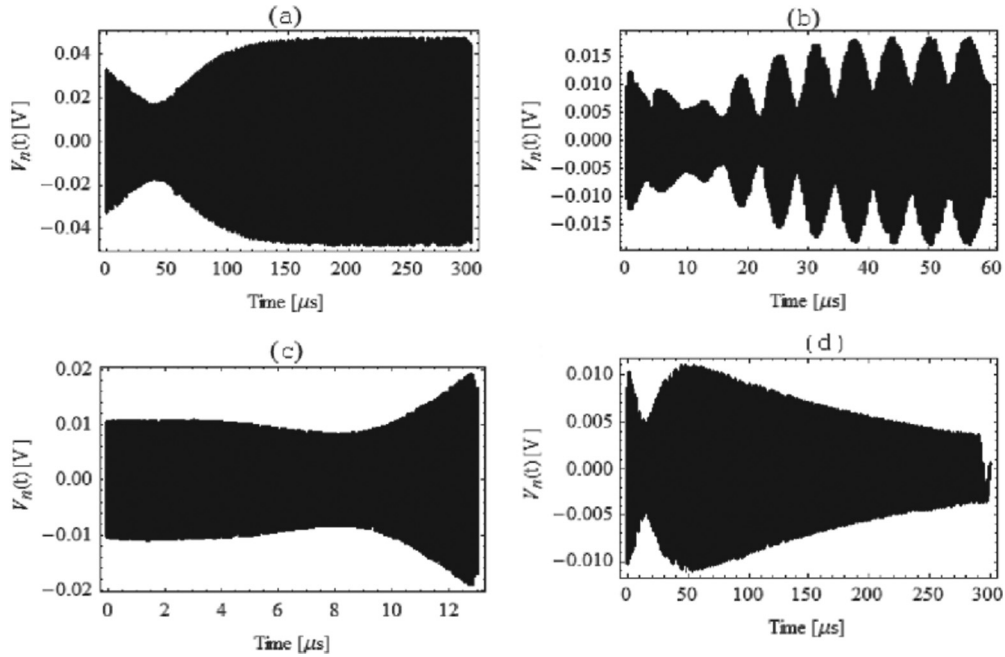


FIG. 7. Propagation of dark soliton in the network at frequency $f = 935.515$ kHz with the network parameters shown in the text for the solution parameters $\varepsilon = 10^{-3}$, $K = -0.1$, $K_0 = 500$, and different functional parameter $\varphi(\tau)$ defined from (a) $\frac{d\varphi(\tau)}{d\tau} = PK^2 + a_0$; (b) $\frac{d\varphi(\tau)}{d\tau} = PK^2 + a_0(1 + 0.5 \cos[\frac{10^6\tau}{\varepsilon^2}])$; (c) $\frac{d\varphi(\tau)}{d\tau} = PK^2 + a_0 \exp[\frac{10^5}{\varepsilon^2}\tau]$; (d) $\frac{d\varphi(\tau)}{d\tau} = PK^2 + a_0 \exp[-\frac{10^5}{\varepsilon^2}\tau]$, where $a_0 = 2000$.

Weierstrass's elliptic function method to derive exact bright, kink, and dark solitary wavelike solutions of the dissipative NLS equation of the network. Using the derived exact solitary waves solutions, we have investigated analytically the dynamics of bright, kink, and dark solitary waves through the network and found the effects of the dissipative elements of the network on the soliton propagation. We have shown

that the wave amplitude decreases while its width increases when the dissipative element of the network increases. We also shown that neither the wave amplitude nor its width varies as the solitary waves propagates along the network. Our investigations show that the dissipative elements of the network can be used to manipulate the motion of bright, kink, and dark solitary waves through the network.

-
- [1] A. C. Newell and J. V. Moloney, *Nonlinear Optics* (Addison-Wesley, New York, 1991).
- [2] A. C. Scott, *Nonlinear Science: Emergence & Dynamics of Coherent Structures* (Oxford University Press, New York, 1999).
- [3] A. Hasegawa, *Optical Solitons in Fibers*, 2nd ed. (Springer, Berlin, 1989).
- [4] D. C. Hutchings and J. M. Arnold, *J. Opt. Soc. Am. B* **16**, 513 (1999).
- [5] A. C. Scott, *Active and Nonlinear Wave Propagation in Electronics* (Wiley-Interscience, New York, 1970).
- [6] R. S. C. Cobbold, *Theory and Application of Field-Effect Transistors* (Wiley, New York, 1970).
- [7] V. P. Popov and T. A. Bickart, *IEEE Trans. Circuits Syst. CAS-21*, 666 (1974).
- [8] A. R. Djordjevic, T. K. Sarkar, and R. F. Harrington, *IEEE Trans. Microwave Theory Tech. MTT-34*, 660 (1986).
- [9] Q. Gu, Y. E. Yang, and J. A. Kong, *J. Electromagn. Waves Appl.* **3**, 183 (1989).
- [10] P. Marquié, J. M. Bilbault, and M. Remoissenet, *Phys. Rev. E* **49**, 828 (1994).
- [11] E. Afshari and A. Hajimiri, *IEEE J. Solid-State Circuits* **40**, 744 (2005).
- [12] E. Kengne, B. Malomed, S. Chui, and W. Liu, *J. Math. Phys.* **48**, 013508 (2007).
- [13] E. Kengne and W. M. Liu, *Phys. Rev. E* **73**, 026603 (2006).
- [14] T. Taniuti and N. Yajima, *J. Math. Phys.* **10**, 1369 (1969).
- [15] E. Kengne, A. Lakhssassi, T. Nguyen-Ba, and R. Vaillancourt, *Can. J. Phys.* **88**, 55 (2010).
- [16] M. Toda, *J. Phys. Soc. Japan* **23**, 501 (1967).
- [17] E. Kengne and N. C. Bame, *Czech. J. Phys.* **55**, 609 (2005).
- [18] E. Kengne, S. T. Chui, and W. M. Liu, *Phys. Rev. E* **74**, 036614 (2006).
- [19] M. Remoissenet, *Waves Called Solitons*, 2nd ed. (Springer, Berlin, 1996).
- [20] L. de Pater and J. W. van den Berg, *Med. Electron. Biol. Eng.* **2**, 161 (1964).
- [21] W. P. Mason, *Electromechanical Transducers and Wave Filters*, 2nd ed. (D. Van Nostrand Co., New York, 1948).
- [22] T. R. Gowrishankar, D. A. Stewart, G. T. Martin, and J. C. Weaver, *BioMed. Eng. OnLine* **3**, 42 (2004).
- [23] H. S. Carslaw and J. C. Jaeger, *Conduction of Heat in Solids*, 2nd ed. (Oxford University Press, Oxford, 1959).

- [24] I. Kokalari, T. Karaja, and M. Guerrisi, *J. Biomed. Sci. Eng.* **6**, 92 (2013).
- [25] A. Noguchi, *Electron. Commun. Jpn.* **57**, 9 (1974).
- [26] T. Yoshinaga and T. Kakutani, *J. Phys. Soc. Jpn.* **53**, 85 (1984).
- [27] D. Yemélé and T. C. Kofané, *J. Phys. D: Appl. Phys.* **39**, 4504 (2006).
- [28] D. Yemélé, P. K. Talla, and T. C. Kofané, *J. Phys. D: Appl. Phys.* **36**, 1429 (2003).
- [29] R. Marquié, J. M. Bilbault, and M. Remoissenet, *Physica D* **87**, 371 (1995).
- [30] J. A. Giannini and R. I. Joseph, *IEEE J. Quantum Electron.* **26**(12), 2109 (1990).
- [31] K. Weierstrass, in *Mathematische Werke V* (Johnson, New York, 1915), pp. 4–16.
- [32] E. T. Whittaker and G. N. Watson, in *A Course of Modern Analysis* (Cambridge University Press, Cambridge, 1927), p. 454.
- [33] H. W. Schürmann, *Phys. Rev. E* **54**, 4312 (1996).